

Article

Electrochemical Sensor for Rapid and Sensitive Detection of Tryptophan by a Cu₂O Nanoparticles-Coated Reduced Graphene Oxide Nanocomposite

Quanguo He ^{1,2,3,†}, Yaling Tian ^{1,2,†}, Yiyong Wu ^{1,2,†}, Jun Liu ¹, Guangli Li ¹, Peihong Deng ^{2,*} and Dongchu Chen ^{3,*}

¹ School of Life Sciences and Chemistry, Hunan University of Technology, Zhuzhou 412007, China; hequanguo@126.com (Q.H.); tianyaling0212@163.com (Y.T.); wyy5082010@163.com (Y.W.); liu.jun.1015@163.com (J.L.); guangli010@hut.edu.cn (G.L.)

² Key Laboratory of Functional Metal–Organic Compounds of Hunan Province, Key Laboratory of Functional Organometallic Materials, University of Hunan Province, Department of Chemistry and Material Science, Hengyang Normal University, Hengyang 421008, China

³ School of Materials Science and Energy Engineering, Foshan University, Foshan 528000, China

* Correspondence: dph1975@163.com (P.D.); chendc@fosu.edu.cn (D.C.); Tel.: +86-731-22183883 (P.D. & D.C.)

† These authors contributed equally to this work.

Received: 3 April 2019; Accepted: 8 May 2019; Published: 8 May 2019



Abstract: In this paper, a nanocomposite of cuprous oxide and electrochemically reduced graphene oxide (Cu₂O–ERGO) was prepared by a simple and low-cost method; hereby, a new method for the electrochemical determination of tryptophan (Trp) by this composite modified glassy carbon electrode (GCE) is proposed. The prepared materials and modified electrodes were characterized by scanning electron microscopy (SEM), X-ray diffraction (XRD), and cyclic voltammetry (CV). The results showed that Cu₂O–ERGO/GCE had good electrocatalytic activity for Trp. The effects of supporting electrolyte, scanning rate, accumulation potential, and accumulation time on the determination of Trp were studied. Under the optimum experimental conditions, Trp was quantitatively analyzed by square-wave voltammetry (SWV). The oxidation peak current of Trp had a good linear relationship with its concentration in the range of 0.02–20 μM, and the detection limit was 0.01 μM (S/N = 3). In addition, the modified electrode has high sensitivity, good repeatability, and long-term stability. Finally, the proposed method has been successfully applied in the determination of Trp concentration in practical samples.

Keywords: cuprous oxide; electrochemical reduced graphene oxide; tryptophan; voltammetric detection

1. Introduction

It is well known that amino acids play an important role in neuroregulation, organ functioning, and metabolism in human beings and animals. Tryptophan (Trp) is an important amino acid that is a precursor of neurotransmitter serotonin and the neurohormone melatonin. It is also essential to the establishment and maintenance of a positive nitrogen balance in human nutrition [1]. Unfortunately, there is an inadequate amount of Trp in vegetables and fruits, and humans and animals cannot synthesize Trp themselves, so Trp must be obtained from food and pharmaceutical formulas. The World Health Organization recommends a Trp intake of 4 mg/kg per day. However, when Trp metabolism malfunctions, toxic waste is produced in the brain, leading to hallucinations and illusions and resulting in neurological dysfunction [2,3]. Therefore, it is important and urgent to establish a simple, sensitive, and selective method for the determination of Trp in food, pharmaceuticals, and living bodies.

So far, there have been many analytical methods for Trp determination, such as high-performance liquid chromatography (HPLC) [4,5], fluorescence [6], capillary electrophoresis [7], chemiluminescence [8], and spectrometry [9]. Although the above methods are useful for the quantitative analysis of Trp, most have the disadvantages of high cost, complicated sample pretreatment process, long response time, and the requirement for human-sized instruments. Electrochemical methods are good choices to solve these defects because of their high accuracy, high sensitivity, simple operation, and low cost. However, the electron transfer process is slow and the overpotential is high for the direct oxidation of Trp on bare electrodes [2]. In addition, some electroactive biomolecules often coexist with Trp in body fluids, which may have a similar oxidation peak potential with Trp and interfere with Trp determination. Chemical modification of electrodes with suitable materials could solve these problems. Therefore, many efforts have been made in recent years to find materials suitable for the design and construction of high-performance electrochemical sensors to reduce the overpotential and improve the sensitivity [10–20]. However, as shown in Table 1, most of them have deficiencies, such as narrow linear range, insufficient low detection limit, or poor stability. The development of enhanced materials and novel sensors for Trp is still of great significance.

Table 1. Comparison of results of Trp sensing between this study and previous reports.

Technique	Modified Electrode	Linear Range (μM)	Detection Limit (μM)	Repeatability (RSD%)	Reproducibility (RSD%)	Stability	Reference
^a DPV	^d EGPU-tAuNP	0.6–2.0	0.053	-	-	-	[10]
DPV	^e β -CD/MWCNTs/GCE	1.5–30.5	0.07	6.0	-	20 days	[11]
DPV	^f ETPG	0.5–50.0	0.05	-	3.2	a month	[12]
	^g PSA/GCE	0.05–10	0.0068	2.7	-	four weeks	[13]
DPV	^h rGO/SnO ₂ /GCE	1–100	0.04	-	2.87	two weeks	[14]
DPV	ⁱ Au-NPs/GCE	0.09–50	0.08	2.4	-	a week	[15]
^b SDLSV	^j Graphene/ABPE	0.1–10; 10–100	0.06	2.7	4.6	two weeks	[16]
amperometry	^k CNF/CPE	0.1–119	0.1	1.0	2.2	an hour	[17]
DPV	^l BuCh/GCE	2–60	0.6	-	-	a month	[18]
DPV	^m MWNTs/GCE	0.25–100	0.027	2.6	-	two weeks	[19]
DPV	ⁿ Pd-Cu@Cu ₂ O/N-RGO/GCE	0.01–40	0.0019	2.11	3.78	a month	[20]
^c SWV	Cu ₂ O-ERGO/GCE	0.02–20	0.01	1.64	4.61	two weeks	This work

^a Differential pulse voltammetry; ^b Second-order derivative linear sweep voltammetry; ^c Square wave voltammetry; ^d Gold nanoparticles modified graphite polyurethane composite electrode; ^e β -cyclodextrin incorporated with multi-walled carbon nanotubes modified glassy carbon electrode; ^f Electrochemically treated pencil graphite electrode (ETPG); ^g Poly(sulfosalicylic acid) modified glassy carbon electrode; ^h Reduced graphene oxide decorated with tin oxide nanoparticles modified glassy carbon electrode; ⁱ Au nanoparticles modified glassy carbon electrode; ^j Graphene modified acetylene black paste electrode; ^k Electrospun carbon nanofibers modified carbon paste electrode; ^l butyrylcholine modified glassy carbon electrode; ^m multi-walled carbon nanotubes modified glassy carbon electrode; ⁿ Pd-Cu@Cu₂O cubes decorated N-doped reduced graphene oxide modified glassy carbon electrode.

Recently, metal oxide nanoparticles have attracted attention in industry and the scientific research field due to their advantages such as high catalysis, low cost, and good stability [21–28]. In recent years, Cu₂O nanoparticles, important p-type semiconductors, have been widely used in solar energy conversion, catalysis, lithium-ion batteries, optical devices, and gas sensors [29–31]. Cu₂O is considered a good additive for composite materials, not only because of its low cost and remarkable catalytic activity, but also because of its good chemical stability, low toxicity, abundance, and easy preparation and functionalization. Up to now, Cu₂O nanoparticles with different morphologies have been synthesized, including nanowire [32], nanooctahedron [33], nanocube [34], and nanosphere [35]. The results show that the structural flexibility of Cu₂O improves its intrinsic electronic and catalytic properties. Graphene, a carbon-based material, is becoming more and more popular as a nanomaterial in electrochemistry due to its unique electronic, chemical, and structural characteristics. Graphene exhibits many excellent properties including high surface area, high conductivity, and low intrinsic size, which makes it attractive as a heterogeneous catalytic matrix [36–38]. Based on these advantages, it has been reported that graphene combined with Cu₂O can be used for electrocatalytic oxidation of dopamine [39,40], hydrogen peroxide [41,42], and glucose [42–44]. These examples confirm that graphene-Cu₂O nanostructures exhibit better catalytic performance in electrochemistry than

single components. The synergistic effect of graphene–Cu₂O may come from the following aspects: (i) electronic coupling between Cu₂O and graphene can greatly improve the catalytic activity; (ii) the conductivity of graphene–Cu₂O composites is higher than when using Cu₂O alone; (iii) Cu₂O can reduce the aggregation of graphene nanosheets and improve the chemical stability with the utilization of catalysts. The incorporation of Cu₂O particles into graphene can improve the electrochemical response of Trp. Therefore, we hope to develop a high-performance electrochemical sensor for Trp.

It is well known that graphene is generally obtained by the chemical reduction of graphene oxide (GO) with hydrazine hydrate or sodium borohydride. However, graphene is hydrophobic. Because of Van der Waals interactions and strong π – π stacking, it often forms irreversible aggregations, which seriously limits its application in electrode modification [16]. Recently the electrochemical reduction of graphene oxide (GO) to produce graphene has been proposed with different electrochemical techniques such as cyclic voltammetry [45,46] or controlled potential method [47,48], which is time-saving, non-toxic, simpler, and greener than chemical reduction methods. Graphene oxide (GO) is a derivative of graphene that has a large specific surface area and many hydrophilic oxygen-containing functional groups on its hydrophobic surface. Such structural characteristics make it a special surfactant and a good carrier to enhance the dispersion of Cu₂O in water. Therefore, Cu₂O nanospheres were prepared using a simple precipitation method and then loaded onto the GO layer. Because the conductivity of GO is poor, the Cu₂O–GO composites were coated on the surface of a glassy carbon electrode (GCE) and reduced by an electrochemical method. The conductivity of electrochemically reduced GO (ERGO) is much higher than that of GO due to the restoration of conductive carbon conjugate networks. It was found that the prepared material had good electrocatalytic activity for Trp. A detailed study was done on the electrochemical behavior of Trp on the Cu₂O–ERGO/GCE. Consequently, a simple, efficient, and low-cost electrochemical method for the rapid and sensitive detection of Trp was proposed.

2. Experimental

2.1. Materials

Cupric sulfate (CuSO₄·5H₂O), tryptophan (Trp), graphite powder, hydrazine hydrate solution (80 wt %), polyvinyl pyrrolidone (PVP) and all other reagents were of analytical grade from Shanghai Sino pharm Chemical Reagent Co. Ltd., Shanghai, China. Compound amino acid injections (17AA-I) and (18AA-I) were obtained from Xuzhou the Fifth Pharmaceutical Corporation, Xuzhou, China and Guangzhou Green Cross Pharmaceutical Corporation, Guangzhou, China, respectively. Buffer and standard solutions were prepared using double distilled water. 1.0 mM Trp solution was prepared by dissolving 0.0204 g Trp in a small volume of 1.0 M NaOH solution, and then diluted with water in a 100-mL volumetric flask. Serial dilutions with doubly distilled water were used to prepare more dilute solutions.

2.2. Apparatus

The electrochemical measurements were performed with a CHI 660E Electrochemical Workstation (Chenhua Instrument Co. Ltd., Shanghai, China). A conventional three-electrode cell was used at room temperature. A Hg/Hg₂Cl₂ (KCl saturated) electrode, a platinum wire electrode, and a bare or modified GCE were used as the reference, auxiliary, and working electrode, respectively. pH measurements were done using a digital pHs-3c Model pH meter (Shanghai Leichi Instrument Factory, Shanghai, China). The morphologies of the nanomaterials were observed by a scanning electron microscope (EVO10, ZEISS, Jena, Germany). The crystal structure of Cu₂O was collected with a powder X-ray diffractometer (PANalytical, Holland, The Netherlands) with Cu K α radiation (0.1542 nm).

2.3. Preparation of Cu₂O and Cu₂O–GO Composites

Cuprous oxide nanoparticles (Cu₂O NPs) were synthesized according to a previous report with some modification [39]. Typically, 100 mg CuSO₄·5H₂O and 50 mg PVP were dissolved in 20 mL H₂O

under stirring. Then 4 mL of 0.2 M NaOH was added dropwise, and blue precipitate was observed. Finally, 15 μ L hydrazine hydrate solution (80 wt %) was added to the above mixture and stirred for 20 min at room temperature and a brick-red suspension resulted. The solid product was separated from the solution by centrifugation, washed with absolute ethanol and water, and dried in vacuum at 60 °C. Graphene oxide (GO) was synthesized referring to our preceding report [16]. Eventually, 1.0 mg of Cu₂O NPs was mixed with 20 mL of GO solution (1 mg/mL), followed by ultrasonication for 2 h to obtain a homogeneous Cu₂O–GO dispersion.

2.4. Preparation of Modified Electrode

To fabricate modified electrode, bare GCE was polished to a mirror-like state by 0.05 μ m α -Al₂O₃ slurry. After successive sonication in ethanol and doubly distilled water, the electrode was allowed to dry at room temperature. Typically, 5 μ L Cu₂O–GO nanocomposite was dropped onto the surface of the cleaned GCE with a micro-injector. The obtained electrode was noted as Cu₂O–GO/GCE. The Cu₂O–GO/GCE was immersed in a 0.1 M phosphate buffer (pH 6.0) and then electrochemically reduced at -1.2 V for 120 s to obtain Cu₂O–ERGO/GCE. In a similar way, GO/GCE, Cu₂O/GCE, and ERGO/GCE were obtained for comparison. When not in use, these modified electrodes were maintained at room temperature.

2.5. Electrochemical Measurements

The electrochemical measurements were performed in a traditional electrochemical cell, which contained a Trp standard solution of known concentration and 0.05 M H₂SO₄ as supporting electrolyte. Accumulation was carried out at -0.1 V for 120 s under continuous stirring, and then kept for 5 s. In the potential range of 0.50–1.1 V, square wave voltammograms were recorded at a scan rate of 0.1 V s⁻¹. After each measurement, the potential scan in the same range was repeated successively 3–5 times in 0.1 M H₂SO₄ solution to refresh the electrode surface.

3. Results and Discussion

3.1. XRD and SEM Characterizations

Figure 1 shows the X-ray diffraction (XRD) patterns of Cu₂O nanoparticles. Diffraction peaks are observed at $2\theta = 29.6^\circ, 36.5^\circ, 42.4^\circ, 61.5^\circ,$ and 73.7° , which are related to (110), (111), (200), (220), and (311) reflections, respectively. The peak positions are consistent with the standard document of Cu₂O (JCPDS No. 05-0667) [49], indicating that the prepared material is crystalline Cu₂O. No diffraction peaks of other possible impurities (such as Cu and CuO) are detected, demonstrating that the product was pure Cu₂O.

The surface morphologies of GO, Cu₂O nanoparticles, ERGO, and Cu₂O–ERGO composites were characterized by a scanning electron microscope (SEM). As shown in Figure 2A, obvious wavy structures could be observed in the SEM image of GO. Figure 2B shows the SEM image of Cu₂O nanoparticles. It was found that Cu₂O nanoparticles are aggregated together, mostly in spherical shape, with an average diameter of about 50–100 nm. As shown in Figure 2C, a lamellar structure of ERGO nanosheets is observed. The layered structure of ERGO can effectively augment the specific surface area of the modified electrode. It can be seen from Figure 2D that a large number of Cu₂O nanoparticles are evenly distributed on the ERGO with lamellar structure, which indicates that Cu₂O nanoparticles are well bound to the ERGO carrier. In addition, the SEM images in Figure 2D show that the morphologies and sizes of Cu₂O nanoparticles are similar to those observed in Figure 2B, showing that the introduction of ERGO does not change the structure of Cu₂O.

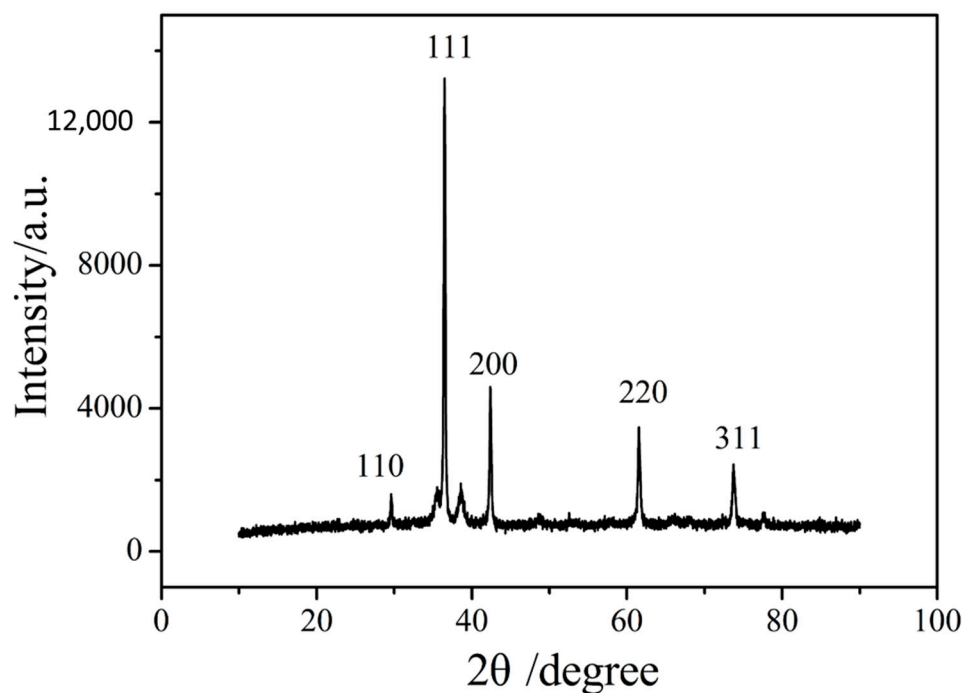


Figure 1. The XRD pattern of Cu_2O nanoparticles.

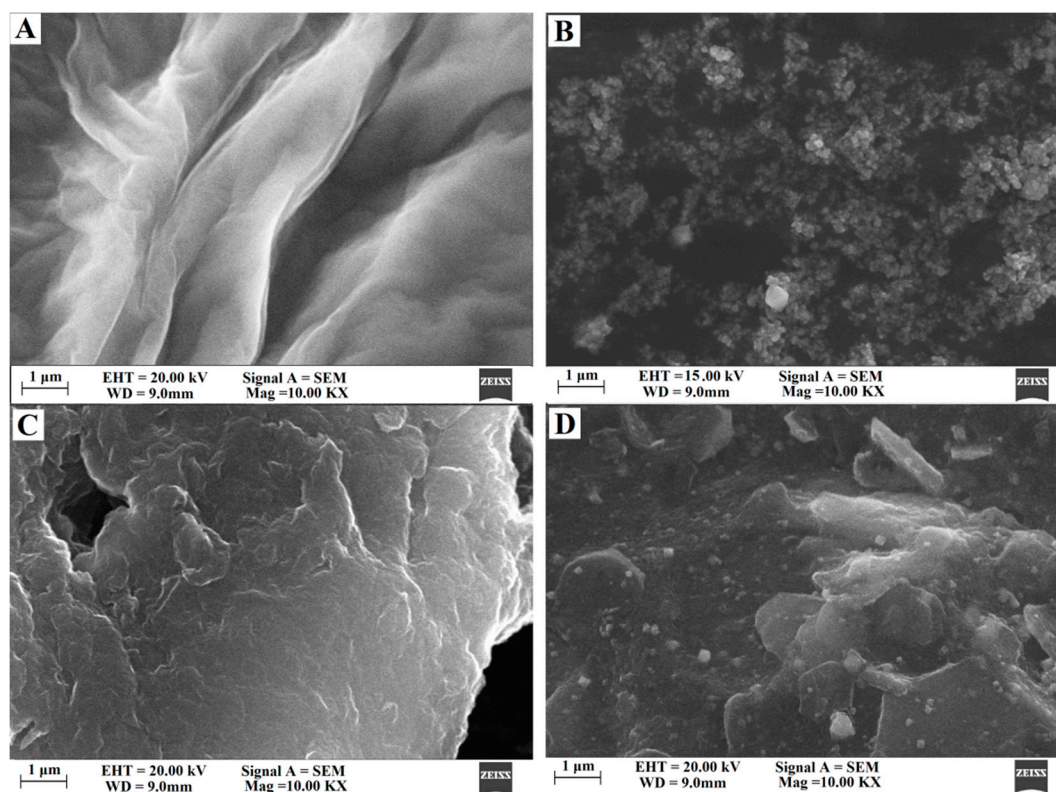


Figure 2. SEM images of (A) GO, (B) Cu_2O nanoparticles, (C) ERGO, and (D) Cu_2O -ERGO composites.

3.2. Electrochemical Characterization of Different Electrodes

Figure 3 shows the cyclic voltammograms of 1 mM $\text{K}_3[\text{Fe}(\text{CN})_6]$ containing 0.5 M KCl at different electrodes in the potential range of -0.2 to 0.8 V. On the GCE (curve a), the peak to peak potential separation (ΔE_p) was 87 mV (vs. SCE) with small redox peak currents, corresponding to a quasi-reversible electron transfer process. On the GO/GCE (curve b), the redox peak current of

$[\text{Fe}(\text{CN})_6]^{3-/4-}$ declines greatly with ΔE_p of 158 mV, which could be due to the weak conductivity of GO. Curve c is the cyclic voltammogram of $\text{K}_3[\text{Fe}(\text{CN})_6]$ obtained at $\text{Cu}_2\text{O}-\text{GO}/\text{GCE}$ with E_{pc} of 0.204 V, E_{pa} of 0.286 V, and ΔE_p of 82 mV. As compared with GO/GCE , the peak currents increase and the peak-to-peak separation decreases obviously. The results indicate that Cu_2O could increase the electron transfer rate of $[\text{Fe}(\text{CN})_6]^{3-/4-}$ due to its excellent catalytic activity. On the ERGO/GCE (curve d), a pair of well-defined redox peaks also appear with the redox peak current increasing and the ΔE_p obviously decreases to 65 mV, which indicates the presence of high conductivity of ERGO. On the $\text{Cu}_2\text{O}-\text{ERGO}/\text{GCE}$ (curve e), the value of ΔE_p is 71 mV with the further increase of the redox peak currents, indicating a more reversible electron transfer process. So, the presence of high conductivity of ERGO together with good catalytic activity of Cu_2O on the GCE surface can further promote the electron transfer and improve the performance of the sensor.

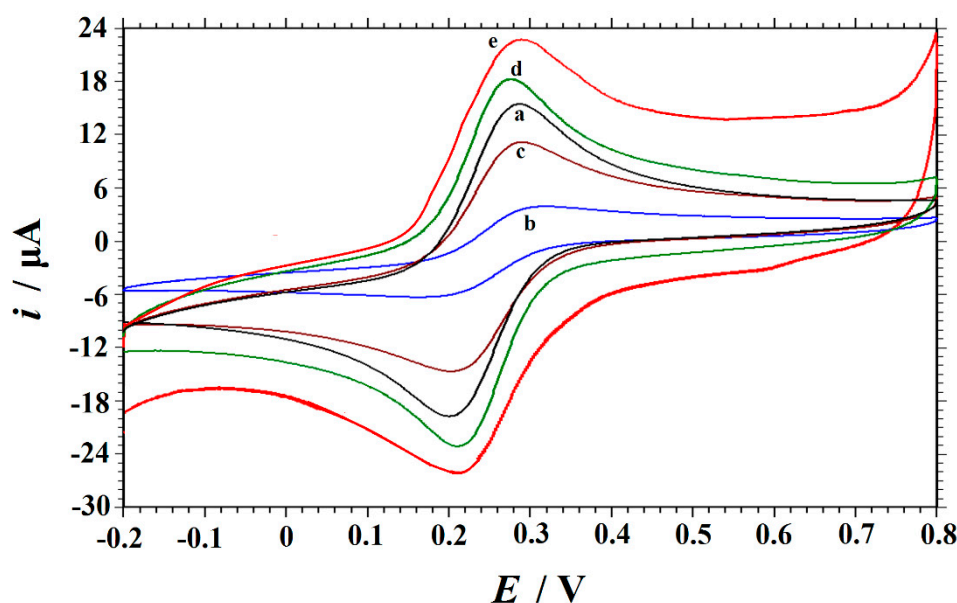


Figure 3. Cyclic voltammograms obtained on (a) GCE, (b) GO/GCE , (c) $\text{Cu}_2\text{O}-\text{GO}/\text{GCE}$, (d) ERGO/GCE and (e) $\text{Cu}_2\text{O}-\text{ERGO}/\text{GCE}$ in a solution of 1.0 mM $\text{K}_3[\text{Fe}(\text{CN})_6]$ and 0.5 M KCl at the scan rate of 0.1 V s^{-1} .

3.3. Voltammetric Behavior of Trp at Different Electrodes

Figure 4 depicts the CV responses of $10 \mu\text{M}$ Trp in $0.05 \text{ M H}_2\text{SO}_4$ solution obtained at different electrodes in a potential range of 0.0 to 1.2 V. As can be seen (inset in Figure 4), no redox peaks are observed at $\text{Cu}_2\text{O}-\text{ERGO}/\text{GCE}$ in a blank solution, indicating that the $\text{Cu}_2\text{O}-\text{ERGO}/\text{GCE}$ is non-electroactive in the selected potential region. On the other hand, when $10 \mu\text{M}$ Trp was added into the blank solution, a well-defined oxidation peak is obtained at $+0.923 \text{ V}$ in the anodic scan, and a small reduction peak is observed at $+0.391 \text{ V}$ in the reverse (cathodic) scan (curve d in Figure 4), which could be attributed to the reduction of the oxidized intermediate of Trp [11]. Table 2 lists the peak potentials and currents of Trp obtained at different electrodes. It is observed that the peak current (i_p) of Trp at ERGO/GCE is about 36 times, three times, and two times higher than that of bare GCE, GO/GCE , and $\text{Cu}_2\text{O}-\text{GO}/\text{GCE}$ respectively, which may be attributed to the high conductivity, large surface area, and good catalytic activity of ERGO. The $\text{Cu}_2\text{O}-\text{ERGO}/\text{GCE}$ shows the largest oxidation peak current compared to other electrodes, which are about 120 times higher than that of the bare GCE and almost three times higher than that of ERGO/GCE . The electrochemical data in Table 2 demonstrate that the order of the ability to accelerate the electron transfer is $\text{Cu}_2\text{O}-\text{ERGO}/\text{GCE} > \text{ERGO}/\text{GCE} > \text{Cu}_2\text{O}-\text{GO}/\text{GCE} > \text{GO}/\text{GCE} > \text{bare GCE}$. The above results suggest that the $\text{Cu}_2\text{O}-\text{ERGO}/\text{GCE}$ combines the excellent properties of Cu_2O and ERGO. Specifically, ERGO has excellent electrical conductivity and

compensates for the deficiency of semiconductor Cu_2O . In addition, ERGO provides a larger specific surface area, which increases the loading of Trp, and Cu_2O immediately exchanges electrons from the Trp loaded in ERGO, promoting the electrocatalytic reaction. Therefore, the nanocomposites can maximize the utilization within a limited electrode surface area, providing an electron transfer microenvironment for accelerating the electrode reaction of Trp and enabling the sensitive determination of Trp.

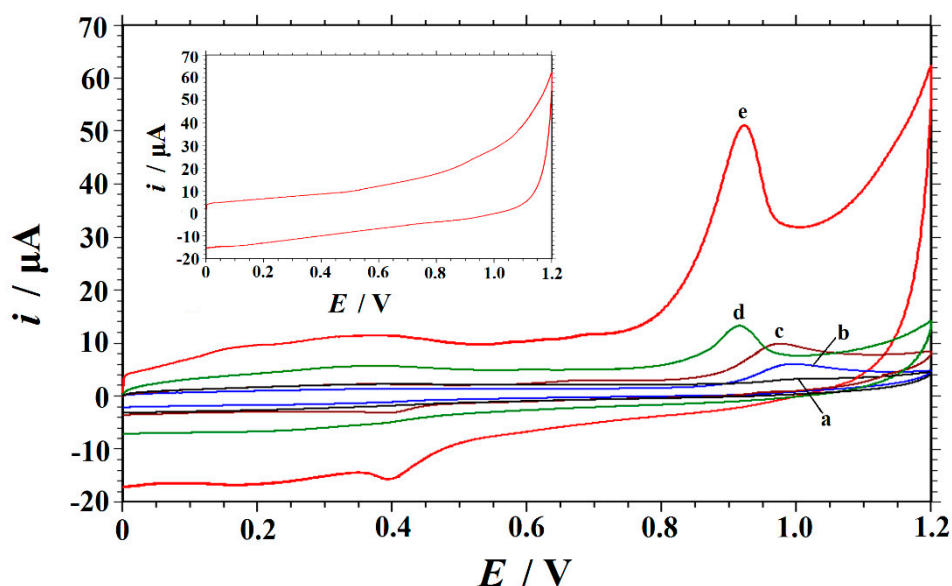


Figure 4. Cyclic voltammograms of 10 μM Trp obtained at different electrodes in 0.05 M H_2SO_4 solution. Curve a: bare GCE; curve b: GO/GCE; curve c: Cu_2O -GO/GCE; curve d: ERGO/GCE; and curve e: Cu_2O -ERGO/GCE. Scan rate: $0.1 \text{ V}\cdot\text{s}^{-1}$. Inset: the cyclic voltammogram of Cu_2O -ERGO/GCE in 0.05 M H_2SO_4 solution.

Table 2. Detailed data of cyclic voltammograms of 10 μM Trp at different electrodes.

Electrode	$i_p/\mu\text{A}$	E_p/V
GCE	0.3190	0.994
GO/GCE	4.295	0.995
Cu_2O -GO/GCE	6.985	0.975
ERGO/GCE	11.48	0.924
Cu_2O -ERGO/GCE	38.17	0.923

3.4. Effect of Scan Rate

The electrode reaction kinetics was studied by investigating the effect of scan rate on the peak current of Trp. Figure 5A indicates the cyclic voltammograms of 10 μM Trp at different scan rates on the Cu_2O -ERGO/GCE. It can be observed that as the scan rate increases from 30 to $300 \text{ mV}\cdot\text{s}^{-1}$, the peak current increases gradually and shows a linear relationship with the scan rate. The linear regression equation can be expressed as $i_p = 162.47 v + 0.5329$ (i_p : μA , v : $\text{V}\cdot\text{s}^{-1}$); the correlation coefficient is $R^2 = 0.9964$, which indicates that the oxidation process of Trp at Cu_2O -ERGO/GCE is an adsorption-controlled process. The adsorption-controlled behavior was also confirmed by plotting $\log i$ vs. $\log v$ corresponding to the equation $\log i = 0.964 \log v + 2.1934$ ($R^2 = 0.9961$). The resulting slope of 0.964 is close to 1.0, confirming the adsorption-controlled properties of the electrode process. As shown in Figure 5C, the peak potential is linearly proportional to the Napierian logarithm of scan rate ($\ln v$) in the range of 30– $300 \text{ mV}\cdot\text{s}^{-1}$, the linear regression equation is $E_p = 0.0237 \ln v + 0.9922$ (E_p : V, v : $\text{V}\cdot\text{s}^{-1}$), with a correlation coefficient of $R^2 = 0.9992$. Based on Laviron's theory [50], the slope of the line is equal to $RT/\alpha nF$, so $\alpha n = 1.08$. It is generally believed that α is 0.5 in the completely irreversible electrode

process [51], so the number of electron transfer (n) involved in the Trp oxidation process is about 2. The results show that at $\text{Cu}_2\text{O-ERGO/GCE}$ two electrons were involved in the oxidation process of Trp.

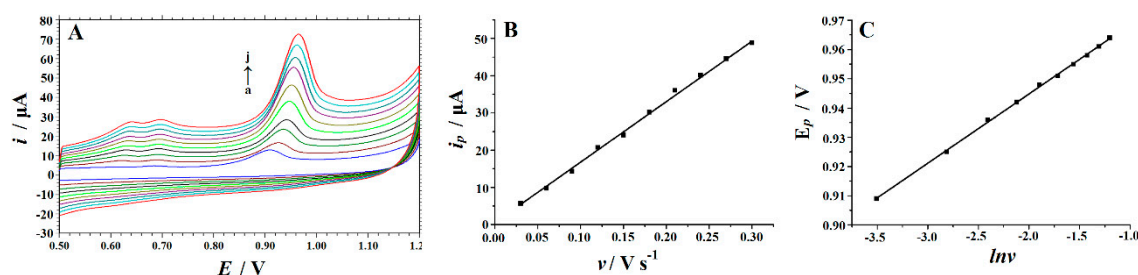


Figure 5. (A) Cyclic voltammograms of 10 μM Trp in 0.05 M H_2SO_4 solution obtained on the $\text{Cu}_2\text{O-ERGO/GCE}$ at different scan rates (a–j: 30, 60, 90, 120, 150, 180, 210, 240, 270, and 300 $\text{mV}\cdot\text{s}^{-1}$). (B) A plot of the peak current versus scan rate; (C) a plot of the peak potential versus the Napierian logarithm of scan rate.

3.5. Optimization of Parameters for Trp Determination

The effects of voltammetric determination parameters on the electrochemical oxidation of Trp were investigated in detail. First, the effect of supporting electrolyte was evaluated by performing the experiments at different supporting electrolyte including Britton–Robinson buffer (pH 3.0–8.0), phosphate buffer (pH 3.0–8.0), HAc-NaAc buffer (pH 3.0–6.0), $(\text{CH}_2)_6\text{N}_4\text{-HCl}$ buffer (pH 3.0–6.0), $\text{HAc-NH}_4\text{Ac}$ buffer (pH 3.0–6.0), $\text{NH}_3\text{-NH}_4\text{Cl}$ (pH 8.0–10.0) and some different acids and alkalis such as H_2SO_4 , HCl , HNO_3 , and NaOH (each 0.1 M). The oxidation peak current values of Trp reached a maximum in H_2SO_4 solution. In addition, the effect of the concentration of H_2SO_4 solution on Trp oxidation was also evaluated in the range from 0.01 M to 0.5 M. It was found that the oxidation peak current of Trp increased with increasing concentration from 0.01 M to 0.05 M, then gradually decreased from 0.05 to 0.5 M (Figure 6). Therefore, 0.05 M H_2SO_4 was used in the current study.

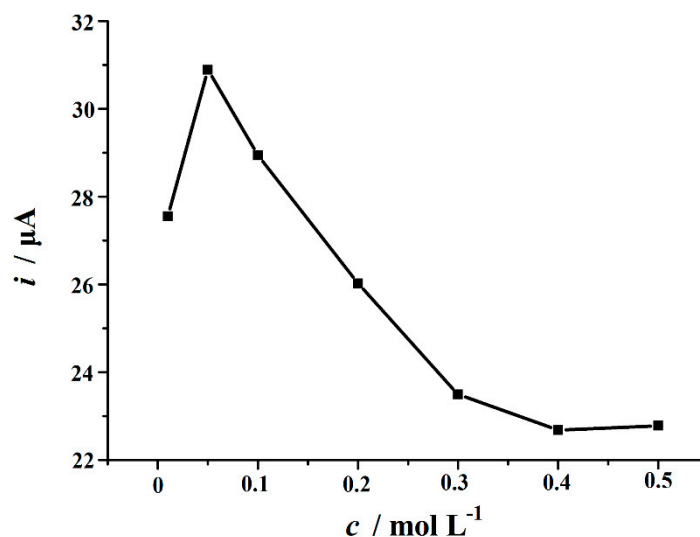


Figure 6. Effect of H_2SO_4 concentration on the oxidation of 10 μM Trp on the $\text{Cu}_2\text{O-ERGO/GCE}$.

The effect of accumulation potential on the peak current was studied in a 10 μM Trp solution at 120 s accumulation time. It could be seen that, as the accumulated potential increased from -0.3 V to -0.1 V, the peak current increased, and then the peak current changed a little with the further positive shift of the accumulation potential (Figure 7A). Therefore, -0.1 V was chosen as the optimal accumulation potential. The effect of accumulation time on the oxidation peak current of Trp was also investigated at -0.1 V. It was found that with the increase of accumulation time, the peak current of

Trp increased gradually. However, beyond 120 s, time period did not lead to significant increment (Figure 7B). Therefore, taking into account the sensitivity together with the analysis speed, 120 s is selected as the optimum accumulation time.

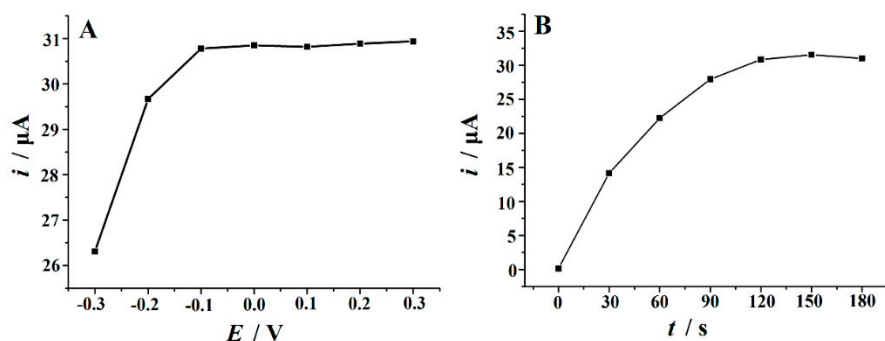


Figure 7. (A) The effect of accumulation potential and (B) accumulation time on the peak current of 10 μM Trp in 0.05M H_2SO_4 solution on the Cu_2O -ERGO/GCE at a scan rate of 100 mV s^{-1} .

3.6. Interference Studies

In this part, the effects of some interfering substances that may present in actual samples on the electrochemical oxidation of Trp were examined. Under the optimal conditions, linear sweep voltammetry (LSV) was performed in 0.05 M H_2SO_4 solution containing 10 μM Trp in the absence and presence of each interfering substance of different concentrations. Ascorbic acid (AA), uric acid (UA), dopamine (DA) usually coexist with Trp in biological fluids. Therefore, the interference effect of AA, UA and DA on the oxidation of Trp was first studied. AA, UA and DA were found to produce oxidation peaks at 235 mV, 468 mV, and 663 mV, separate from the Trp peak (Figure 8). The experimental results showed that the peak current response of Trp did not change significantly in the presence of 100-fold excess of AA, 20-fold excess of UA and DA. In addition, the effects of other different species were also studied. No substantial changes in the peak current of Trp were observed in the presence of 100-fold excess of glucose, tartaric acid, citric acid, sodium chloride, and potassium chloride. Moreover, in biological fluids as well as some pharmaceutical preparations, Trp often coexists with different amino acids. Therefore, we separately studied the interference effects of different amino acids. Since most amino acids are not electroactive, it was found that 100-fold concentrations of glycine, alanine, valine, leucine, isoleucine, phenylalanine, histidine, and glutamic acid had no effect on Trp oxidation (signal change $\leq \pm 5.0\%$). However, the oxidation peak potential of tyrosine is very close to that of Trp. The results show that 2-fold tyrosine has no obvious interference on the determination of Trp.

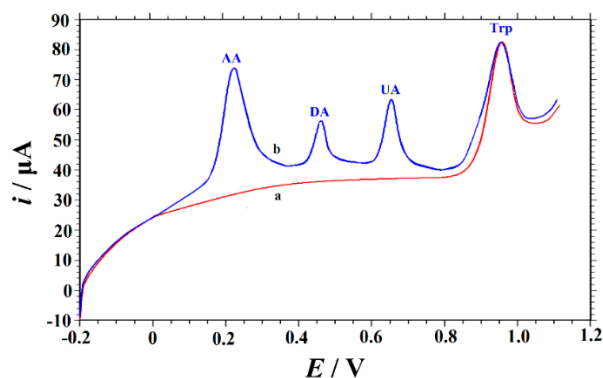


Figure 8. Linear sweep voltammograms of 10 μM Trp in 0.05 M H_2SO_4 solution on the Cu_2O -ERGO/GCE in the absence of (curve a) and presence of 1.0 mM AA, 10 μM dopamine (DA), and 10 μM uric acid (UA) (curve b). Accumulation potential: -0.1 V , accumulation time: 120 s, scan rate: 100 mV s^{-1} .

3.7. Calibration Curve and Limit of Detection

Under the optimized conditions, Trp was quantitatively analyzed by square wave voltammetry (SWV), and the corresponding voltammograms of different concentrations of Trp in the range of 0.02 μM to 20 μM are shown in Figure 9A. The oxidation peak current increased linearly with Trp concentration. The calibration curve of Trp measurement (Figure 9B) showed a linear relationship with Trp concentration (0.02–20 μM). The regression equation is $i_p (\mu\text{A}) = 3.1596c (\mu\text{M}) + 0.4811$ ($R^2 = 0.9992$). The low detection limit can be calculated by using Equation (1):

$$\text{LOD} = 3s_b/S. \quad (1)$$

In the formula, s_b is the standard deviation of seven blank measurements and S is the sensitivity. The low detection limit was identified at 0.01 μM ($S/N = 3$). The linear range and detection limit of $\text{Cu}_2\text{O-ERGO/GCE}$ were compared with other electrodes. As indicated in Table 1, the linear range obtained on $\text{Cu}_2\text{O-ERGO/GCE}$ was comparable to and even wider than that of other modified electrodes, and the detection limit was lower than that of most electrodes except PSA/GCE [12] and $\text{Pd-Cu@Cu}_2\text{O/N-RGO/GCE}$ [20]. Although a better detection limit (1.9 nM) and a wider linear range (0.01–40 μM) have been achieved on $\text{Pd-Cu@Cu}_2\text{O/N-RGO/GCE}$, the noble metal Pd was used for electrode preparation. In addition, hydrothermal synthesis and chemical reduction were used in the preparation of the electrode. Due to the high cost of Pd and the complex and time-consuming preparation process, its practical application in commercial uses is greatly restricted. These results show that $\text{Cu}_2\text{O-ERGO/GCE}$ is a suitable platform for Trp determination. In addition, compared with other carbon-based materials, $\text{Cu}_2\text{O-ERGO/GCE}$ has the advantages of low production costs and a simple preparation method.

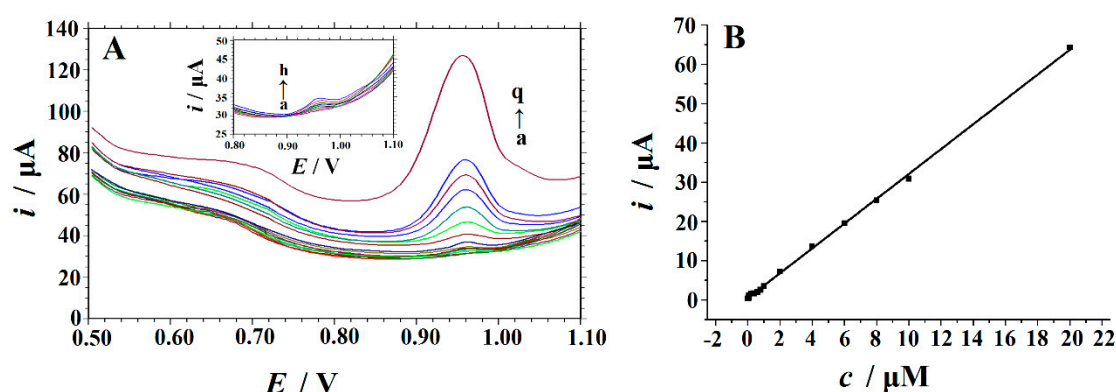


Figure 9. (A) SWVs of different concentrations of Trp (a→q: 0.02, 0.04, 0.06, 0.08, 0.1, 0.2, 0.4, 0.6, 0.8, 1.0, 2.0, 4.0, 6.0, 8.0, 10, and 20 μM) on the $\text{Cu}_2\text{O-ERGO/GCE}$ in 0.05 M H_2SO_4 solution at a scan rate of 100 mV s^{-1} . Inset: magnified image of the curve a→h. (B) The linear relationship between the i_p and Trp concentration in the range of 0.02–20 μM . Accumulation potential: -0.1 V ; accumulation time: 120 s.

3.8. Repeatability, Reproducibility, and Stability of $\text{Cu}_2\text{O-ERGO/GCE}$

According to some reports [13–15], Trp is easily adsorbed onto the electrode surface and fouls the electrodes. In the present work, the most attractive feature of measuring Trp using $\text{Cu}_2\text{O-ERGO/GCE}$ is that the electrode surface is easily renewed for the next use. After each measurement, the used electrode was rinsed in 0.1 M H_2SO_4 solution and several voltammetric scans in the potential range of 0.5–1.2 V were carried out. The relative standard deviation (RSD) of seven measurements on the same electrode in a 10 μM Trp solution was 1.64%, which indicated the weak adsorption of Trp oxidation product on the electrode surface. In order to demonstrate the stability of $\text{Cu}_2\text{O-ERGO/GCE}$, 100 CVs were performed using 10 μM Trp. It was found that the peak current decreased only 3.47% even after 100 cycles. We also demonstrated the reproducibility by measuring the CV changes in a 10 μM Trp

solution obtained on seven different electrodes, and the RSD was calculated to be 4.61%. Furthermore, Cu₂O-ERGO/GCE long-term stability was also tested. The experimental results showed that the current response of the modified electrode was 94.28% after two weeks in the refrigerator, which indicates that the modified electrode has high stability.

3.9. Practical Applications

To explore the application feasibility of Cu₂O-ERGO/GCE in the determination of Trp, human serum samples and commercial compound amino acid injections were used as real samples. Before analysis, serum samples were prepared according to our previous report [52], then the compound amino acid injection was diluted 100 times with double-distilled water. Thereafter, an aliquot of the sample solutions was diluted with 0.05 M H₂SO₄. In order to prevent the matrix effect, a standard addition method was used. The results are shown in Table 3. The recoveries of human serum samples and amino acid injection samples were 97.0–102.3% and 98.0–101.2%, respectively. The results indicated that the electrode had high selectivity and accuracy for the determination of Trp in drugs and biological samples.

Table 3. Determination of Trp in real samples ($n = 4$).

Samples	Labeled/ μM	^a Detected/ μM	Added/ μM	^a Total Detected/ μM	Recovery/%
17AA-I	2.12	2.14 (± 0.06)	2.0	4.10 (± 0.10)	98.0
18AA-I	4.90	4.97 (± 0.13)	5.0	10.03 (± 0.29)	101.2
Serum 1	-	1.29 (± 0.03)	1.0	2.26 (± 0.06)	97.0
Serum 2	-	2.74 (± 0.07)	1.0	5.81 (± 0.15)	102.3

^a Average \pm confidence interval, the confidence level is 95%.

4. Conclusions

A highly sensitive electrochemical method was established for the determination of Trp by Cu₂O-ERGO/GCE. On Cu₂O-ERGO/GCE, Trp undergoes a sensitive oxidation process and a sharp peak is observed. The oxidation enhancement of Trp is due to the synergistic effect of Cu₂O and ERGO on the surface of the electrode. The results show that the modified electrode has wide linear range, low detection limit, high stability, and good selectivity for the determination of Trp. In addition, the modified electrode has the advantages of good reproducibility and simple preparation, especially its anti-fouling performance to Trp and its oxidation product. The method has been applied to the determination of Trp in human serum samples and commercial amino acid injections. The results indicate that the method can be applied for the determination of Trp concentration in real samples.

Author Contributions: P.D., D.C., and Q.H. conceived and designed the experiments; Y.W., Y.T., J.L., and G.L. performed the experiments; P.D. and Y.T. analyzed the data; D.C. and Q.H. contributed reagents/materials/analysis tools; Q.H. and P.D. wrote the paper.

Funding: This work was supported by the NSFC (61703152), Hunan Provincial Natural Science Foundation (2016JJ4010, 2018JJ3134), the Postgraduate Innovation Fund of the School of Life Sciences and Chemistry in HUT, the Doctoral Program Construction of Hunan University of Technology, Project of Science and Technology of Hunan Province Education Department (18A273, 18C0522), the Project of Science and Technology Plan in Zhuzhou (201706-201806), Opening Project of Key Discipline of Materials Science in Guangdong (ESI Project GS06021, CNXY2017001, CNXY2017002 and CNXY2017003), the Key Project of the Department of Education of Guangdong Province (2016GCZX008), the Foundation of Key Laboratory of Functional Organometallic Materials, University of Hunan Province, the Foundation of Key Laboratory of Functional Metal–Organic Compounds of Hunan Province and a project of the Engineering Research Center of Foshan (20172010018).

Conflicts of Interest: The authors declare no conflict of interest.

References

1. Gholivand, M.B.; Pashabadi, A.; Azadbakht, A.; Menati, S.A. nano-structured Ni(II)–ACDA modified gold nanoparticle self-assembled electrode for electrocatalytic oxidation and determination of tryptophan. *Electrochim. Acta* **2011**, *56*, 4022–4030. [[CrossRef](#)]
2. Babaei, A.; Zendejdel, M.; Khalilzadeh, B.; Taheri, A. Simultaneous determination of tryptophan, uric acid and ascorbic acid at iron(III) doped zeolite modified carbon paste electrode. *Colloids Surf. B Biointerfaces* **2008**, *66*, 226–232.
3. He, Q.; Liu, J.; Liang, J.; Liu, X.; Li, W.; Liu, Z.; Ding, Z.; Tuo, D. Towards Improvements for Penetrating the Blood–Brain Barrier—Recent Progress from a Material and Pharmaceutical Perspective. *Cells* **2018**, *7*, 24. [[CrossRef](#)] [[PubMed](#)]
4. Zhang, L.; Li, Y.; Zhou, H.; Li, L.; Wang, Y.; Zhang, Y. Determination of eight amino acids in mice embryonic stem cells by precolumn derivatization HPLC with fluorescence detection. *J. Pharm. Biomed. Anal.* **2012**, *66*, 356–358. [[CrossRef](#)]
5. Dario, M.F.; Freire, T.B.; de Oliveira Pinto, C.A.S.; Prado, M.S.A.; Baby, A.R.; Velasco, M.V.R. Tryptophan and kynurenine determination in human hair by liquid chromatography. *J. Chromatogr. B* **2017**, *1065–1066*, 59–62. [[CrossRef](#)]
6. Jiao, L.; Bing, S.; Zhang, X.; Wang, Y.; Li, H. Determination of enantiomeric composition of tryptophan by using fluorescence spectroscopy combined with backward interval partial least squares. *Anal. Methods* **2015**, *7*, 4535–4540. [[CrossRef](#)]
7. Gomez, F.J.; Martin, A.; Silva, M.F.; Escarpa, A. Microchip electrophoresis-single wall carbon nanotube press-transferred electrodes for fast and reliable electrochemical sensing of melatonin and its precursors. *Electrophoresis* **2015**, *36*, 1880–1885. [[CrossRef](#)] [[PubMed](#)]
8. Lin, Z.J.; Chen, X.M.; Cai, Z.M.; Li, P.W.; Chen, X.; Wang, X.R. Chemiluminescence of tryptophan and histidine in Ru(bpy)₃²⁺-KMnO₄ aqueous solution. *Talanta* **2008**, *75*, 544–550. [[CrossRef](#)] [[PubMed](#)]
9. Lee, C.J.; Yang, J. α -Cyclodextrin-modified infrared chemical sensor for selective determination of tyrosine in biological fluids. *Anal. Biochem.* **2006**, *359*, 124–131.
10. Mattioli, I.A.; Baccarin, M.; Cervini, P.; Cavalheiro, É.T.G. Electrochemical investigation of a graphite-polyurethane composite electrode modified with electrodeposited gold nanoparticles in the voltammetric determination of tryptophan. *J. Electroanal. Chem.* **2019**, *835*, 212–219. [[CrossRef](#)]
11. Mukdasai, S.; Poosittisak, S.; Ngeontae, W.; Srijaranai, S. A highly sensitive electrochemical determination of L-tryptophan in the presence of ascorbic acid and uric acid using in situ addition of tetrabutylammonium bromide on the β -cyclodextrin incorporated multi-walled carbon nanotubes modified electrode. *Sens. Actuators B Chem.* **2018**, *272*, 518–525. [[CrossRef](#)]
12. Özcan, A.; Şahin, Y. A novel approach for the selective determination of tryptophan in blood serum in the presence of tyrosine based on the electrochemical reduction of oxidation product of tryptophan formed in situ on graphite electrode. *Biosen. Bioelectron.* **2012**, *31*, 26–31. [[CrossRef](#)] [[PubMed](#)]
13. Ba, X.; Luo, L.; Ding, Y.; Liu, X. Determination of l-tryptophan in the presence of ascorbic acid and dopamine using poly(sulfosalicylic acid) modified glassy carbon electrode. *Sens. Actuators B Chem.* **2013**, *187*, 27–32. [[CrossRef](#)]
14. Haldorai, Y.; Yeon, S.-H.; Huh, Y.S.; Han, Y.-K. Electrochemical determination of tryptophan using a glassy carbon electrode modified with flower-like structured nanocomposite consisting of reduced graphene oxide and SnO₂. *Sens. Actuators B Chem.* **2017**, *239*, 1221–1230. [[CrossRef](#)]
15. Li, C.; Ya, Y.; Zhan, G. Electrochemical investigation of tryptophan at gold nanoparticles modified electrode in the presence of sodium dodecylbenzene sulfonate. *Colloids Surf. B Biointerfaces* **2010**, *76*, 340–345. [[CrossRef](#)] [[PubMed](#)]
16. Deng, P.; Xu, Z.; Feng, Y. Acetylene black paste electrode modified with graphene as the voltammetric sensor for selective determination of tryptophan in the presence of high concentrations of tyrosine. *Mater. Sci. Eng. C* **2014**, *35*, 54–60. [[CrossRef](#)] [[PubMed](#)]
17. Tang, X.; Liu, Y.; Hou, H.; You, T. Electrochemical determination of L-Tryptophan, L-Tyrosine and L-Cysteine using electrospun carbon nanofibers modified electrode. *Talanta* **2010**, *80*, 2182–2186. [[CrossRef](#)]
18. Jin, G.P.; Lin, X.Q. The electrochemical behavior and amperometric determination of tyrosine and tryptophan at a glassy carbon electrode modified with butyrylcholine. *Electrochem. Commun.* **2004**, *6*, 454–460. [[CrossRef](#)]

19. Wu, F.-H.; Zhao, G.-C.; Wei, X.-W.; Yang, Z.-S. Electrocatalysis of tryptophan at multi-walled carbon nanotube modified electrode. *Microchim. Acta* **2004**, *144*, 243–247. [[CrossRef](#)]
20. Li, J.; Jiang, J.; Xu, Z.; Liu, M.; Tang, S.; Yang, C.; Qian, D. Facile synthesis of Pd–Cu@Cu₂O/N-RGO hybrid and its application for electrochemical detection of tryptophan. *Electrochim. Acta* **2018**, *260*, 526–535. [[CrossRef](#)]
21. He, Q.; Liu, J.; Liu, X.; Li, G.; Chen, D.; Deng, P.; Liang, J. Fabrication of amine-modified magnetite-electrochemically reduced graphene oxide nanocomposite modified glassy carbon electrode for sensitive dopamine determination. *Nanomaterials* **2018**, *8*, 194. [[CrossRef](#)]
22. He, Q.; Li, G.; Liu, X.; Liu, J.; Deng, P.; Chen, D. Morphologically tunable MnO₂ nanoparticles fabrication, modelling and their influences on electrochemical sensing performance toward dopamine. *Catalysts* **2018**, *8*, 323. [[CrossRef](#)]
23. Elhag, S.; Ibupoto, Z.H.; Liu, X.; Nur, O.; Willander, M. Dopamine wide range detection sensor based on modified Co₃O₄ nanowires electrode. *Sens. Actuators B Chem.* **2014**, *203*, 543–549. [[CrossRef](#)]
24. He, Q.; Liu, J.; Liu, X.; Li, G.; Deng, P.; Liang, J.; Chen, D. Sensitive and selective detection of tartrazine based on TiO₂-Electrochemically reduced graphene oxide composite-modified electrodes. *Sensors* **2018**, *18*, 1911. [[CrossRef](#)]
25. Carbone, M.; Nesticò, A.; Bellucci, N.; Micheli, L.; Palleschi, G. Enhanced performances of sensors based on screen printed electrodes modified with nanosized NiO particles. *Electrochim. Acta* **2017**, *246*, 580–587. [[CrossRef](#)]
26. He, Q.; Wu, Y.; Tian, Y.; Li, G.; Liu, J.; Deng, P.; Chen, D. Facile electrochemical sensor for nanomolar rutin detection based on magnetite nanoparticles and reduced graphene oxide decorated electrode. *Nanomaterials* **2019**, *9*, 115. [[CrossRef](#)]
27. He, Q.; Liu, J.; Liu, X.; Li, G.; Deng, P.; Liang, J. Manganese dioxide Nanorods/electrochemically reduced graphene oxide nanocomposites modified electrodes for cost-effective and ultrasensitive detection of Amaranth. *Colloids Surf. B Biointerfaces* **2018**, *172*, 565–572. [[CrossRef](#)]
28. He, Q.; Liu, J.; Liu, X.; Li, G.; Chen, D.; Deng, P.; Liang, J. A promising sensing platform toward dopamine using MnO₂ nanowires/electro-reduced graphene oxide composites. *Electrochim. Acta* **2019**, *296*, 683–692. [[CrossRef](#)]
29. Akimoto, K.; Ishizuka, S.; Yanagita, M.; Nawa, Y.; Paul, G.K.; Sakurai, T. Thin film deposition of Cu₂O and application for solar cells. *Sol. Energy*. **2006**, *80*, 715–722. [[CrossRef](#)]
30. Poizot, P.; Laruelle, S.; Grugeon, S.; Dupont, L.; Tarascon, J.M. Nano-sized transition-metal oxides as negative-electrode materials for lithium-ion batteries. *Nature* **2000**, *407*, 496–499. [[CrossRef](#)]
31. Zhang, H.; Zhu, Q.; Zhang, Y.; Wang, Y.; Zhao, L.; Yu, B. One-Pot Synthesis and Hierarchical Assembly of Hollow Cu₂O Microspheres with Nanocrystals-Composed Porous Multishell and Their Gas-Sensing Properties. *Adv. Funct. Mater.* **2007**, *17*, 2766–2771. [[CrossRef](#)]
32. Singh, D.P.; Ali, N. Synthesis of TiO₂ and CuO nanotubes and nanowires. *Sci. Adv. Mater.* **2010**, *2*, 295–335. [[CrossRef](#)]
33. Ng, S.Y.; Ngan, A.H.W. Fabrication of nanometer-to-micron sized Cu₂O single crystals by electrodeposition. *Electrochim. Acta* **2011**, *56*, 7686–7695. [[CrossRef](#)]
34. Gou, L.; Murphy, C.J. Controlling the size of Cu₂O nanocubes from 200 to 25 nm. *J. Mater. Chem.* **2004**, *14*, 735–738. [[CrossRef](#)]
35. Zhang, J.T.; Liu, J.F.; Peng, Q.; Wang, X.; Li, Y.D. Nearly monodisperse Cu₂O and CuO nanospheres: Preparation and applications for sensitive gas sensors. *Chem. Mater.* **2006**, *18*, 867–871. [[CrossRef](#)]
36. He, Q.; Tian, Y.; Wu, Y.; Liu, J.; Li, G.; Deng, P.; Chen, D. Facile and Ultrasensitive Determination of 4-Nitrophenol Based on Acetylene Black Paste and Graphene Hybrid Electrode. *Nanomaterials* **2019**, *9*, 429. [[CrossRef](#)]
37. Deng, P.; Xu, Z.; Zeng, R.; Ding, C. Electrochemical behavior and voltammetric determination of vanillin based on an acetylene black paste electrode modified with grapheme–polyvinylpyrrolidone composite film. *Food Chem.* **2015**, *180*, 156–163. [[CrossRef](#)]
38. Li, J.; Xu, Z.; Liu, M.; Deng, P.; Tang, S.; Jiang, J.; Feng, H.; Qian, D.; He, L. Ag/N-doped reduced graphene oxide incorporated with molecularly imprinted polymer: An advanced electrochemical sensing platform for salbutamol determination. *Biosens. Bioelectron.* **2017**, *90*, 10–216. [[CrossRef](#)]

39. He, Q.; Liu, J.; Liu, X.; Li, G.; Deng, P.; Liang, J. Preparation of Cu₂O-reduced graphene nanocomposite modified electrodes towards ultrasensitive dopamine detection. *Sensors* **2018**, *18*, 199. [[CrossRef](#)]
40. Zhang, F.; Li, Y.; Gu, Y.; Wang, Z.; Wang, C. One-pot solvothermal synthesis of a Cu₂O/Graphene nanocomposite and its application in an electrochemical sensor for dopamine. *Microchim. Acta* **2011**, *173*, 103–109. [[CrossRef](#)]
41. Xu, F.; Deng, M.; Li, G.; Chen, S.; Wang, L. Electrochemical behavior of cuprous oxide–reduced graphene oxide nanocomposites and their application in nonenzymatic hydrogen peroxide sensing. *Electrochim. Acta* **2013**, *88*, 59–65. [[CrossRef](#)]
42. Li, Y.; Zhong, Y.; Zhang, Y.; Weng, W.; Li, S. Carbon quantum dots/octahedral Cu₂O nanocomposites for non-enzymatic glucose and hydrogen peroxide amperometric sensor. *Sens. Actuators B* **2015**, *206*, 735–743. [[CrossRef](#)]
43. Cao, H.; Yang, A.; Li, H.; Wang, L.; Li, S.; Kong, J.; Bao, X.; Yang, R. A non-enzymatic glucose sensing based on hollow cuprous oxide nanospheres in a Nafion matrix. *Sens. Actuators B* **2015**, *214*, 169–173. [[CrossRef](#)]
44. Yuan, B.; Xu, C.; Liu, L.; Zhang, Q.; Ji, S.; Pi, L.; Zhang, D.; Huo, Q. Cu₂O/NiO_x/graphene oxide modified glassy carbon electrode for the enhanced electrochemical oxidation of reduced glutathione and nonenzyme glucose sensor. *Electrochim. Acta* **2013**, *104*, 78–83. [[CrossRef](#)]
45. Shao, Y.; Wang, J.; Engelhard, M.; Wang, C.; Lin, Y. Facile and controllable electrochemical reduction of graphene oxide and its applications. *J. Mater. Chem.* **2010**, *20*, 743–748. [[CrossRef](#)]
46. Chen, L.; Tang, Y.; Wang, K.; Liu, C.; Luo, S. Direct electrodeposition of reduced graphene oxide on glassy carbon electrode and its electrochemical application. *Electrochem. Commun.* **2011**, *13*, 133–137. [[CrossRef](#)]
47. Guo, H.L.; Wang, X.F.; Qian, Q.Y.; Wang, F.B.; Xia, X.H. A green approach to the synthesis of graphene nanosheets. *ACS Nano* **2009**, *3*, 2653–2659. [[CrossRef](#)] [[PubMed](#)]
48. Unnikrishnan, B.; Mani, V.; Chen, S.-M. Highly sensitive amperometric sensor for carbamazepine determination based on electrochemically reduced graphene oxide–single-walled carbon nanotube composite film. *Sens. Actuators B* **2012**, *173*, 274–280. [[CrossRef](#)]
49. Long, J.; Dong, J.; Wang, X.; Ding, Z.; Zhang, Z.; Wu, L.; Li, Z.; Fu, X. Photochemical synthesis of submicron- and nano-scale Cu₂O particles. *J. Colloid Interface Sci.* **2009**, *333*, 791–799. [[CrossRef](#)]
50. Laviron, E. Adsorption, autoinhibition and autocatalysis in polarography and in linear potential sweep voltammetry. *J. Electroanal. Chem.* **1974**, *52*, 355–393. [[CrossRef](#)]
51. Hu, S.; Wu, K.; Yi, H.; Cui, D. Voltammetric behavior and determination of estrogens at Nafion-modified glassy carbon electrode in the presence of cetyltrimethylammonium bromide. *Anal. Chim. Acta* **2002**, *464*, 209–216. [[CrossRef](#)]
52. Deng, P.; Fei, J.; Feng, Y. Sensitive voltammetric determination of tryptophan using an acetylene black paste electrode modified with a Schiff's base derivative of chitosan. *Analyst* **2011**, *136*, 5211–5217. [[CrossRef](#)]

